Wavelength Optimization in Femtosecond Laser Corneal Surgery

Caroline Crotti,[1] Florent Deloison,[*,1] Fatima Alahyane,[1] Florent Aptel,[2] Laura Kowalczuk,[1] Jean-Marc Legeais,[3] Donald A. Peyrot,[1] Michèle Savoldelli,[3] and Karsten Plamann[1]

[1]Laboratoire d'Optique Appliquée, ENSTA ParisTech, École Polytechnique, Palaiseau, France
[2]Service d'Ophtalmologie, CHU de Grenoble, Hôpital A. Michallon, Grenoble, France
[3]Laboratoire Biotechnologie et Œil, Université Paris Descartes/hôpital Hôtel-Dieu, Paris, France

Correspondence: Karsten Plamann, Laboratoire d'Optique Appliquée, ENSTA ParisTech – École Polytechnique – CNRS UMR 7639, 828 boulevard des Maréchaux, 91762 Palaiseau cedex, France; Karsten.Plamann@ensta-paristech.fr.

Current affiliation: *ALPhANOV, Talence, France

Submitted: August 2, 2012
Accepted: March 15, 2013

Citation: Crotti C, Deloison F, Alahyane F, et al. Wavelength optimization in femtosecond laser corneal surgery. *Invest Ophthalmol Vis Sci.* 2013;54:3340–3349. DOI:10.1167/iovs.12-10694

Purpose. To evaluate the influence of wavelength on penetration depth and quality of femtosecond laser corneal incisions in view of optimizing procedures in corneal surgery assisted by ultrashort pulse lasers.

Methods. We performed penetrating and lamellar incisions on eye bank corneas using several ultrashort pulse laser sources. Several wavelengths within the near-infrared and shortwave-infrared wavelength range were used and the pulse energy was varied. The corneas were subsequently analyzed using light microscopy as well as transmission and scanning electron microscopy.

Results. We found higher penetration depths and improved incision quality when using wavelengths close to $\lambda = 1650$ nm rather than the wavelength of $\lambda = 1030$ nm typical in current clinical systems. Optical micrographs show an improvement of the penetration depth by a factor of 2 to 3 while maintaining a good incision quality when using the longer wavelength. These results were confirmed with micrographs obtained with transmission and scanning electron microscopy.

Conclusions. A wavelength change from the standard 1030 nm to 1650 nm in corneal surgery assisted by ultrashort pulse laser considerably reduces light scattering within the tissue. This results in a better preservation of the laser beam quality in the volume of the tissue, particularly when working at depths required for deep lamellar or penetrating keratoplasty. Using this wavelength yields improved penetration depths into the tissue; it permits use of lower energies for any given depth and thus reduces unwanted side effects as thermal effects.

Keywords: cornea, keratoplasty, transparency, laser, surgery

The purpose of the present study is to evaluate the influence of wavelength on penetration depth and quality of femtosecond (fs) laser corneal incisions, in order to identify the optimal wavelength for ultrashort pulse laser surgery of the cornea. Results will provide information for potential developments of improved clinical systems.

The subtle nonlinear interaction process of ultrashort laser pulses with matter permits strongly localized modifications in the volume of transparent matter and makes them potentially very useful for different forms of surgery.[1] Laboratory experiments have been performed since the 1980s.[2–7] Development of clinical systems did not become conceivable,[8] however, until compact, diode-pumped ultrashort pulse laser sources became available toward the end of the 1990s. The first clinical application of femtosecond laser systems was in refractive surgery, where they are used to create the corneal flap during LASIK (laser in situ keratomileusis[9,10]). In recent years, the use of femtosecond lasers for LASIK rather than the mechanical microkeratome has become increasingly widespread. Most LASIK systems also offer routines for keratoplasty; new systems for cataract surgery are currently being commercialized (for reviews, see Salomão and Wilson, Soong and Malta, and Plamann et al.[11–13]). The available clinical lasers typically work with infrared laser pulses wavelengths just above 1 μm and yield good, reproducible results when used on healthy and therefore clear corneas. However, most indications for keratoplasty are associated with a strongly reduced optical transparency of the tissue that is caused by increased light scattering in edematous or otherwise pathological tissue (Plamann et al.[13]). Performing deep lamellar or penetrating cuts can be difficult in the volume of those corneas; incomplete dissections with residual tissular bridges are often observed.[14–16]

The present study suggests that a change of laser wavelength permits improved surgical results. The nonlinear interaction process of femtosecond laser pulses with the tissue itself, which permits the creation of the surgical incisions, does not depend strongly on the wavelength. Olivié and coworkers studied the influence of the wavelength on ablation threshold—that is, the minimal radiant exposure that is sufficient to create optical breakdown and residual incisions—at the surface of porcine corneal stroma, with pulses of wavelength ranging from 800 to 1450 nm and a pulse duration of 100 fs.[17] This study concludes that the ablation threshold slightly increases with increasing wavelength until 1000 nm where it reaches a plateau. Beyond this wavelength, the threshold is supposed to be quite constant and remains close to a radiant exposure of about 2.2 J/cm^2.

In the following, we will show experimental results that demonstrate the benefit of using wavelengths close to 1650 nm, notably in terms of penetration depth and quality of the surgical incisions.

Transparency of Healthy and Edematous Cornea

Light scattering in cornea is closely linked to the tissular micro- and nanostructure.[18,19] In healthy cornea with intact epithelium and endothelium, the residual scattering is dominated by scattering processes in the volume of the stroma that represents about 80% of the corneal thickness. The stroma is organized in collagen lamellae of micrometric thicknesses constituted of collagen fibrils with distances of several 10 nm. Two light-scattering mechanisms may be identified in the stroma: the strongly wavelength-dependent "Rayleigh" scattering caused by the collagen fibrils, and scattering processes caused by objects with micrometric dimensions like keratocytes, which show little wavelength dependence. In healthy cornea, Rayleigh scattering is minimized by a very regular local arrangement of the fibrils; scattering by keratocytes and other objects of micrometric dimensions is equally low. In edematous cornea, the fibril arrangement becomes irregular, which increases Rayleigh scattering. In the case of severe edema, regions devoid of collagen fibrils called "lakes" may appear. While both of these phenomena considerably increase light scattering, the overall scattering process remains strongly wavelength-dependent, which suggests that a change of the laser wavelength may help to reduce the influence of scattering and overcome the aforementioned problems.[13]

In order to optimize beam quality and penetration depth in the volume of the tissue, one needs to find the optimal tradeoff between reducing light scattering by increasing wavelength and light absorption by water molecules that have strong absorption bands in the shortwave infrared (SWIR) spectral region. Sacks et al.[20,21] studied the wavelength dependence of spot size, penetration depth, and optical breakdown in the volume of scleral tissue at wavelengths ranging from 1100 nm to 2600 nm and observed improved penetration depth and beam quality at wavelengths close to 1700 nm where a local minimum in the water absorption spectrum exists.

We have performed detailed measurements of the fraction of directly transmitted light—that is, photons having experienced little or no deviation—and the total light transmission of healthy and edematous cornea.[22] Figure 1 shows a typical result of our transparency measurements we have described in detail elsewhere. Transmission loss below about 600 nm may be attributed to backscattered light; the principal tissular components of the cornea are not light absorbing in this wavelength range. Above about 900 nm, the contributions of several water absorption bands become visible in the spectrum with a very pronounced absorption peak centered at about 1450 nm.[23] This total transmission may be compared with the "direct" transmission that we define as forward-transmitted photons remaining close to the optical axis within a solid angle of 10^{-7} sr. We observe that the direct transmission efficiency increases with wavelength until it experiences water absorption. We also observe that within a spectral window centered at 1650 nm, the direct transmission dominates and accounts almost completely for total transmission. Within this spectral range around 1650 nm, the transmitted light experiences very little light scattering.

We repeated this experiment on a number of eye bank corneas prepared to different degrees of edema by an osmotic deswelling treatment.

Figure 2 gives an overview of our experimental results by plotting the percentage of scattered light as a function of the thickness (degree of edema) for different wavelengths. ("scattered" in this case means deviated out of a solid angle of 10^{-7} sr in the forward direction; see Ref. 22 for details.) In short, our results show the following:

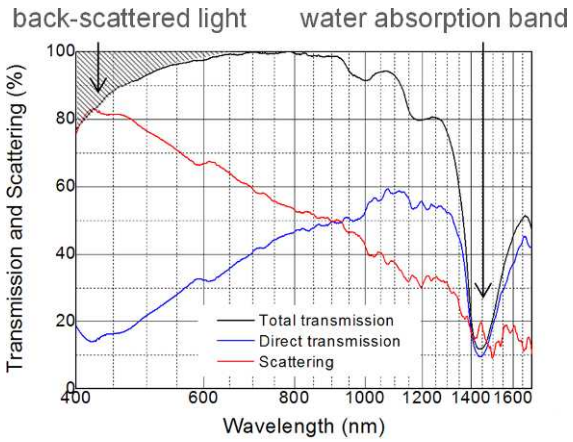

Figure 1. Transmission and scattering spectra for a mildly edematous cornea: total transmission (*black line*), direct transmission (*blue line*), and scattered light (*red line*).

- For all wavelengths, the strength of the light scattering in cornea depends strongly on thickness. Light scattering decreases with decreasing thickness until a minimum is reached at about 480 μm, which corresponds to the physiological thickness of healthy corneas (with removed epithelium), which suggests that the corneal tissue is naturally optimized for transparency. Further thinning of the cornea increases light scattering.[22]
- As predicted by theory, light scattering in all corneas decreases very strongly with increasing wavelength.

Specifically, even for very edematous cornea, at a wavelength of 1650 nm, about 60% of the transmitted photons remain within a solid angle of 10^{-7} sr. Our conclusions for cornea are similar to the ones of Sacks et al.[20,21] for sclera. Our results show that, while scattering is strong within the visible spectral range, a spectral window of relative optical transparency centered at 1650 nm exists in the cornea, within which the transmitted light experiences very little light scattering. We

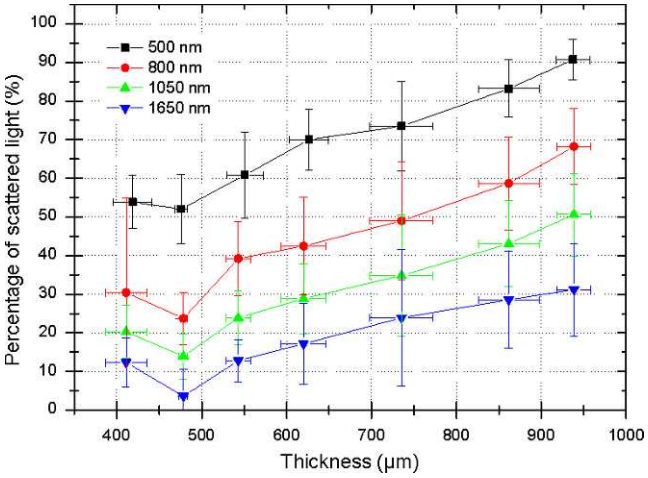

Figure 2. Percentage of light scattered by human corneas as a function of thickness (degree of edema) and wavelength (data partly taken from Peyrot et al.[22]).

could therefore assume that the use of laser wavelengths close to 1650 nm would improve penetration depth and incision quality in cornea. At this wavelength, the overall transparency is mainly absorption limited. Given the improvement of the beam quality, this could in principle be compensated by a slight increase in pulse energy, but it has to be verified experimentally that no unwanted thermal side effects occur during surgery.

Materials and Methods

Laser System

Three laser systems have been used for the present study:

- Source 1 is a powerful but complex laboratory system, which requires the infrastructure and qualified personnel of a research laboratory for operation. It is a commercial optical parametric amplifier (OPA) system (Palitra; Quantronix, East Setauket, NY) pumped by a laboratory titanium-sapphire laser. This pump laser emits mJ pulses at a central wavelength close to 813 nm and a repetition rate of 1 kHz with pulse durations of 30 to 40 fs at the output of the laser. In this configuration, two different successive crystals amplify a "super continuum" (white light) signal. The system emits pulses tunable between 1000 and 2000 nm at energies up to about 100 μJ at a repetition rate of 1 kHz with pulse lengths of well below 100 fs.
- Source 2 is a commercial diode-pumped solid state laser (DPSSL; s-Pulse HP; Amplitude Systèmes, Pessac, France). In the configuration used for our experiments, it emits 600 fs pulses at 1030 nm at a repetition rate of 10 kHz. The system is compact, rugged, and its parameters are equivalent to those of clinical femtosecond laser systems.
- Source 3, based on source 2, has been specially developed by our group to provide a compact and rugged laser instrument potentially adapted to clinical use at higher wavelengths (around 1650 nm). It is a single-pass optical parametric generator (OPG) composed of a crystal of periodically polarized lithium locate doped with magnesium (PPMLN; HC Photonics, Hsinchu, Taiwan). The OPG temperature is maintained by an electrical oven at adjustable values between 60°C and 200°C, and optical pumping is provided by source 2's commercial DPSSL. The length of the period within the PPMLN crystal determines the central output wavelength. Several structures are available in each individual crystal giving access to an overall tuning range of 1460 to 2000 nm for 600 fs pulses. At a repetition rate of 10 kHz, we obtain maximum pulse energies of about 20 μJ. It has to be noted that this system has an emission bandwidth of up to 200 nm, which is relatively large compared with the other two used in this study. The resulting system remains well adapted to potential clinical use at modified wavelengths; overall simplicity, size, and ruggedness are comparable with source 2.

Sample Preparation, Experimental Setup, and Protocol

The study was conducted according to the tenets of the Declaration of Helsinki and the French legislation for scientific use of human corneas. Human corneas unsuitable for transplantation because of low endothelial cell density or an insufficient size of the optical zone (<8 mm) were obtained from the *Banque Française des Yeux* (French Eye Bank, Paris, France). Corneoscleral disks were stored using the organ culture technique in CorneaMax medium (Eurobio, Courtabœuf, France). Storage time ranged from 13 to 15 days; storage typically promotes swelling so that the corneas used for the experiments presented here were mildly or strongly edematous.

A schematic view of the experimental setup is shown in Figure 3. The corneas were placed on the artificial chamber shown (K20-2125 Barron Artificial Anterior Chamber; Katena Products, Inc, Denville, NJ), filled with BSS. The thickness of each cornea was measured by ultrasound pachymetry (Pocket II; Quantel Medical, France). We then placed a standard microscope coverslip on the surface of the cornea in order to obtain a flat surface. The coverslip has a thickness of about 170 μm, a refractive index of 1.44 to 1.45, and a transmission of more than 90%, which varies very little within the considered spectral range. It may therefore be considered having physical properties similar to those of the applanation lenses used with clinical systems. The laser is focused into the tissue using one of two microscope objectives (Zeiss Plan NeoFluar ×20, numerical aperture (NA) = 0.4; and Nachet Plan Apochromat, NA = 0.57). The chamber may be positioned using an XYZ step motor module (Newport Inc., Irvine, CA). The laser exposure and the incision routine are controlled by homemade software using a commercial programming language (LabView; National Instruments, Austin, TX). The laser parameters were monitored by an autocorrelator (PulseCheck; APE GmbH, Berlin, Germany); a spectrometer (NIRQuest256-2.5; Ocean Optics Inc., Dunedin, FL); and a powermeter (UP19K-15S-H5-D0; Gentec Electro Optics, Inc., Québec, Canada).

Experimental Protocol

In principle, almost any cut geometry may be programmed. The first part of this study focuses on incisions perpendicular to the corneal surface, which best monitor the preservation—or degradation—of the laser beam quality in the volume of the tissue. The cuts have been performed by focusing the laser at the endothelial side and then moving upward toward the epithelial side of the cornea. As soon as the available radiant exposure is sufficient to reach the optical breakdown threshold, the laser-tissue interaction induces a cut in the tissue. The step motor's scanning speed was adjusted to position individual pulses at distances of 2 to 3 μm, to ensure that continuous cuts at threshold are obtained. As the physical processes causing optical breakdown are mostly deterministic, the depth measurement at which breakdown occurs is a good metric for beam

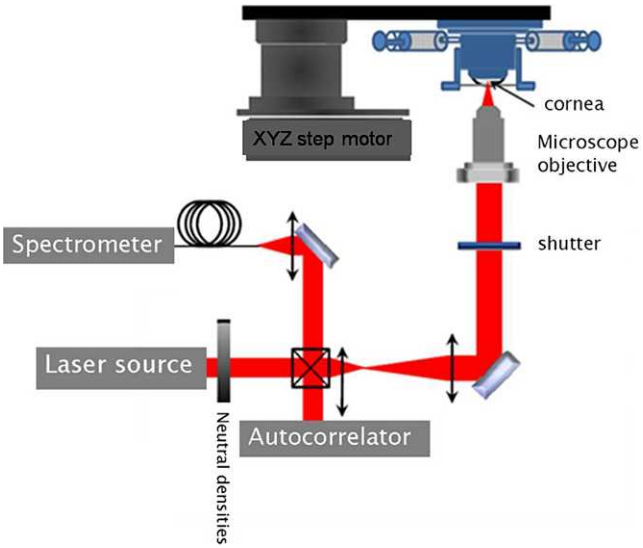

Figure 3. Experimental setup to perform incisions.

quality evolution in the sample volume. We have performed several series of incisions using focusing optics with two different numerical apertures (0.4 and 0.57) while varying wavelength, pulse energies, and laser system; the incision lengths were measured from histological cuts (see below).

The second part of the study aims to evaluate the quality of lamellar cuts and its dependence on laser parameters. Automated routines were programmed permitting to perform laser cuts corresponding to the dimensions and thickness of LASIK flaps and geometries for anterior keratoplasty, except for the cut outlines. These rectangular shapes (as opposed to the circular or oval shapes typical for LASIK and keratoplasty) were chosen in order to avoid possible positioning artifacts at the flap circumference caused by the step motor system, which is optimized for rectilinear movements. Using different wavelengths, horizontal ("lamellar") cuts parallel to the corneal surface were first introduced at a fixed depth; penetrating cuts were then performed at three sides of their circumference up to the corneal surface to give access to the lamellar incision.

The samples were then examined by scanning electron microscopy (SEM).

Sample Analysis

After the laser procedure, the corneas were fixed in 2.5% glutaraldehyde cacodylate buffer (0.1 M, pH 7.4). Specimens were additionally fixed in 1% osmium tetroxyde in cacodylate buffer (0.2 M, pH 7.4) and subjected to successive dehydration in graduated ethanol solution (50%, 70%, 95%, and 100%) then in propylene oxide. Each area of interest was separately included in epoxy resin and oriented. Semi-thin sections (1 μm) were obtained with an ultramicrotome (OmU2; Reichert, Vienna, Austria) and stained with toluidine blue for histological observation with an optical microscope. Ultra-thin sections (80 nm) were contrasted by uranyl acetate, and analyzed with a transmission electron microscope (CM10, Philips, The Netherlands).

Lamellar cuts were examined by SEM in a specialized laboratory after being dehydrated and coated with a thin gold layer.

Results

Penetrating Cuts

Evaluation of the Penetration Depth. Figure 4 shows a histological section of penetrating incisions performed in an edematous cornea (thickness $d \approx 1$ mm) at wavelengths of $\lambda =$ 1030 nm using source 2 (commercial DPSSL) and at 1450 nm, 1500 nm, 1550 nm, 1600 nm, 1650 nm, and 1700 nm using source 3 (OPG) . The numerical aperture used was 0.57, and pulse energy was $E = 2$ μJ with individual pulses positioned at a 3-μm distance from each other. The incision length is strongly wavelength-dependent; no cuts are possible with satisfactory quality at wavelengths within the water absorption band. Thermal effects become visible notably at the absorption peak centered at 1450 nm. This and similar experiments typically yield a factor of ≥2 improvement of cut depth at given pulse energy by changing the wavelength from 1030 nm (as used by clinical systems) to 1650 nm, which we consider optimal for strongly light scattering cornea.

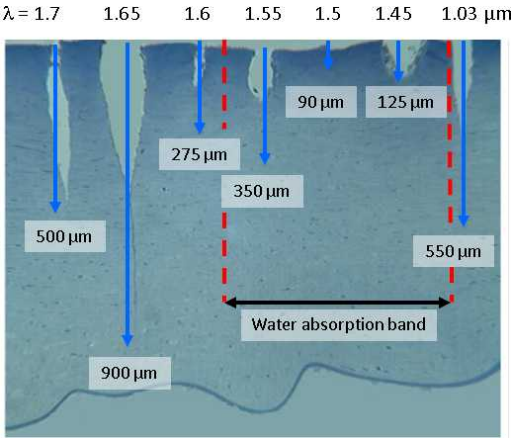

Figure 4. Incisions performed in an edematous cornea at NA = 0.57 and $E = 2$ μJ using different wavelengths obtained from the DPSSL (source 2, 1.03 μm) and the OPG (source 3, other wavelengths).

This improvement is apparent in results shown in Figure 5. On the left, the figure shows incisions performed at those two wavelengths in an edematous cornea while varying the pulse energy. The resulting incision lengths are plotted on the right: for this particular experiment, at any given pulse energy the incision length obtained using the wavelength of $\lambda = 1650$ nm is typically twice the one obtained at 1030 nm.

Although it is obviously difficult to predict and quantify the behavior of the surgical laser beam in the volume of tissue specimens with varying properties, we may still make an estimate for the dependence of the beam attenuation of the wavelength. We may assume that the evolution of the radiant exposure W as a function of the depth z in the volume of the sample roughly follows a Lambert-Beer law

$$W(z) = W_0 \cdot e^{-\frac{z}{l}} \quad (1)$$

where W_0 is the unperturbed radiant exposure, reached when

Table 1. Overview Over the Laser Sources Used for the Surgical Experiments

	Max. Pulse Energy, μJ (unless indicated otherwise)	Wavelength Tunability, nm	Spectral Bandwidth, nm	Repetition Rate, kHz	Pulse Duration, fs
Commercial OPA*	~100	1000–2000	180 (50 using bandpass filters)	1	~50
Commercial DPSSL (oscillator + regenerative amplifier)†	200 (at 10 kHz)‡	1030	4	10§	600
OPG² pumped by the precedent source||	~20	1460–2000	Up to 200	10	~600

* Palitra, Quantronix, East Setauket, NY.
† S-pulse HP, Amplitude Systèmes, Pessac, France.
|| Crystal supplied by HC Photonics, Hsinchu, Taiwan.
‡ Since the publication of Ref. 13, we have obtained maximum output energies of about 20 μJ for a one-crystal configuration.
§ The repetition rate of this laser can be chosen between 1 kHz and 100 kHz; the highest pulse energy is obtained at 1 kHz. For the experiments reported in this paper, we used the parameters indicated here.

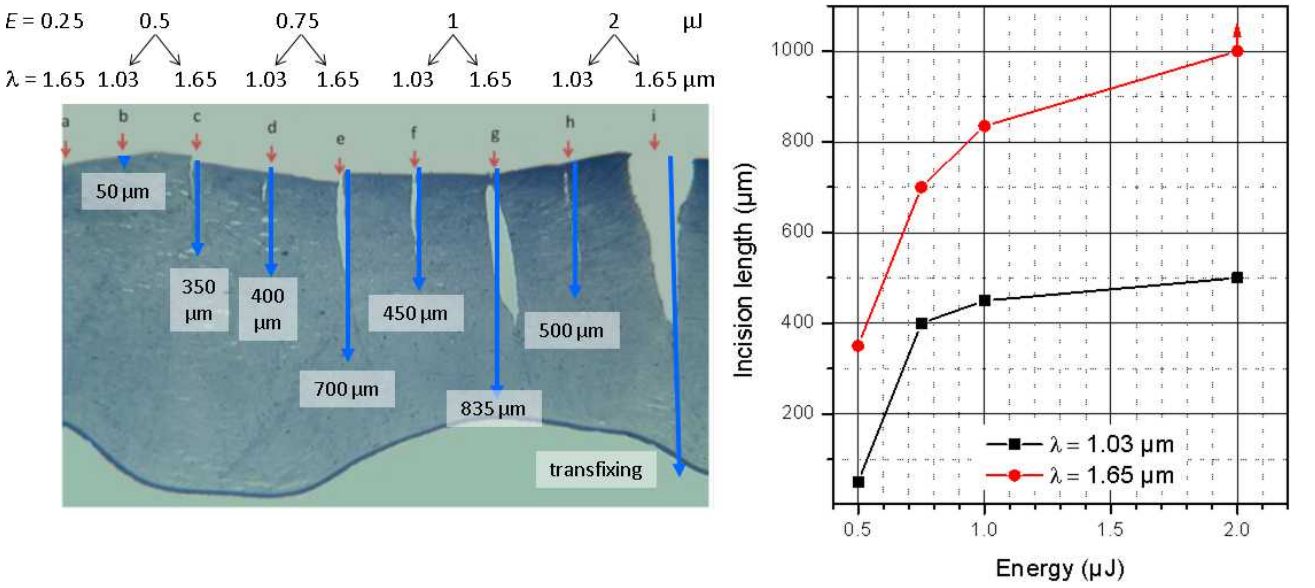

Figure 5. Analysis of the maximum incision depth human cornea induced by a femtosecond laser as a function of pulse energy and laser wavelength. *Left*: Histological section showing incisions performed at NA = 0.57 at 1.03 µm and 1.65 µm using pulse energies between 0.25 µJ (only a superficial cut was produced) and 2 µJ (OPG, source 3) on an edematous cornea of an average thickness of about 900 µm. *Right*: incision lengths obtained from the histological section; lines are guides for the eye. Logarithmic fits to data obtained from this and comparable experiments yielded the penetration depths plotted in Figure 6.

the focal spot is placed at the surface of the sample, and ℓ is the $1/e$ penetration depth. The term ℓ may serve as a penetration depth metric in the cornea (see, for instance, Nuzzo et al.[24]). If we define W_{th} as the threshold radiant exposure (which we assume here being little dependent on other experimental parameters), we may calculate ℓ from the maximum incision length z_{th} until which the threshold is reached as

$$z_{th} = \ell \cdot \ln\left(\frac{W_0}{W_{th}}\right) \quad (2)$$

Thus, ℓ may be obtained by a logarithmic numerical fit of data as shown in Figure 5 (right) using this equation. We note that this method does not require knowledge of the actual value of W_{th}.

Incisions with varying energy were performed at different wavelengths on corneas ($n = 12$) presenting varying degrees of edema. The penetration depth ℓ was estimated using numerical fits of Equation 2 to the data. The data obtained is summarized in Table 2 and plotted in Figure 6 as a function of the wavelength. Note that laser source 2 is used as reference at 1030 nm as mentioned before and for longer wavelengths, both laser sources 1 and 3 have been used.

The data shows the expected tendency: penetration depths for thicker and thus more edematous corneas are generally inferior to less edematous specimens. For comparable corneas, the wavelength change toward the transparency window centered at 1650 nm resulted in an improvement in penetration depth of typically about 2 to 3.

Based on these results, we do not conclude that numerical aperture has significant influence on penetration depth within

Table 2. Penetration Depths Obtained by Fitting the Parameters of Equation 2 to Data Obtained From 12 Experiments of the Type Shown in Figure 5

Source	Wavelength, nm	Corneal Thickness, µm	Numerical Aperture	Penetration Depth/ SD (µm)
2	1030	650	0.57	226 (71)
2	1030	680	0.4	112 (27)
2	1030	680	0.57	96 (23)
2	1030	950	0.4	90 (4)
1	1280	950	0.4	204 (51)
1	1590	900	0.4	223 (32)
1	1592	800	0.4	391 (107)
1	1592	900	0.4	300 (54)
1	1600	800	0.57	269 (65)
3	1650	650	0.57	664 (29)
3	1650	950	0.57	483 (73)
1	1700	900	0.4	270 (51)

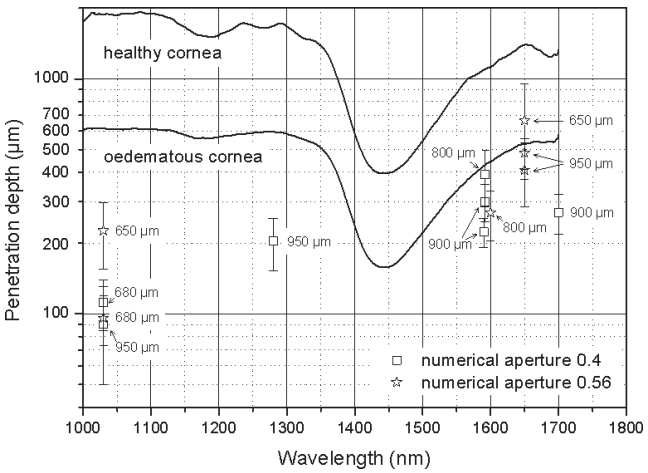

Figure 6. Penetration depth ℓ of the surgical laser beam plotted as a function of the wavelength (data shown in Table 2). The labels close to the symbols indicate the thickness of the cornea. For comparison purposes, we have plotted penetration depths as obtained from optical transparency measurements for a typical healthy and an edematous cornea (*solid lines*, see text for discussion).

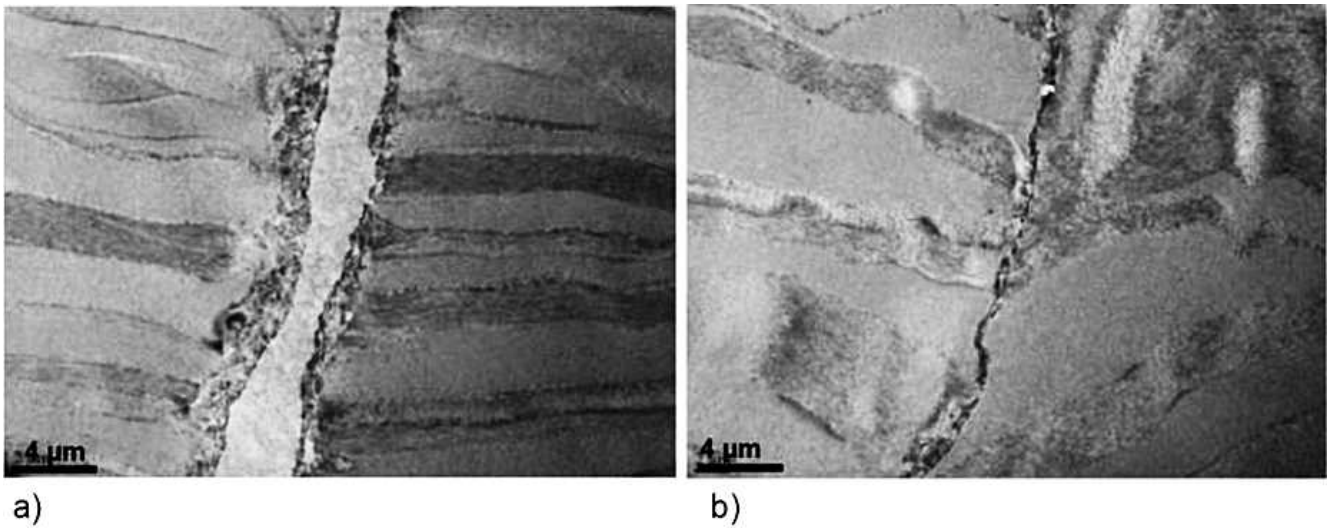

FIGURE 7. Typical transmission electron micrographs of incisions performed in the volume of the stroma at wavelengths of (**a**) 1030 nm and (**b**) 1650 nm using a DPSSL (source 2) and an OPG (source 3) on the same cornea using 2 µJ pulses and a numerical aperture of 0.57.

our experimental parameters. We attribute this to broadening effects due to light scattering processes in the volume of the cornea, which dominate spot size effects linked to the numerical apertures used. This trend is also supported by the considerable penetration depth improvement observed with increasing wavelength, despite the resulting spot size increase, and reduced radiant exposure (assuming diffraction limited beam quality).

Analysis of the Incision Quality by Transmission Electron Microscopy. In an earlier work, we presented a study of transfixing incisions performed using NIR wavelengths examined by transmission electron microscopy (TEM) showing the remarkable cut quality.[25] For the present work, we have to verify that surgical result are not degraded due to thermal side effects caused by optical absorption in water and other tissue components. Figure 7 shows two typical transmission electron micrographs of incisions using 1650 nm wavelength pulses. We observe that the tissular structure remains unperturbed except at the borders of the incisions, and in particular the disrupted collagen fibers' organization was preserved, without signs of thermal or mechanical damage. The average fibril diameter and interfibrillar distances remained constant across the corneal stroma.

Lamellar Cuts

We present here lamellar cuts performed with laser sources 1 (1600 nm and 1650 nm) and source 2 (reference wavelength, 1030 nm). A total of five corneas was used.

Manual Detachment of the Flaps and Observation of Tissular Bridges. To demonstrate cut quality and depth dependence on wavelength, we performed two series of cuts. The first, with source 2, at a wavelength of $\lambda = 1030$ nm, was made at depths of 140 µm and 190 µm using pulse energies of 2, 4, and 8 µJ; a numerical aperture of 0.4; and a pulse spacing of 1 or 2 µm. The second, with source 1, at pulse energies and wavelengths of 1 µJ/1600 nm and 2 µJ/1650 nm, respectively, used a numerical aperture of 0.4. The reader may compare these conditions with the experiment shown in Figure 5, where we observed that pulse energies of 2 µJ should be sufficient to perform incisions throughout the thickness of the cornea using a wavelength of 1650 nm, and up to a depth of about 500 µm when using 1030 nm. The chosen conditions should therefore permit to perform continuous, uninterrupted lamellar cuts. When possible, the flap was then manually opened to observe flap detachment and the possible presence of residual tissular bridges. Table 3 gives an overview of the results obtained.

TABLE 3. Experimental Conditions Used for the Lamellar Incisions and Indications About the Facility of the Flap Detachment and the Presence of Residual Tissular Bridges

Source	Wavelength, nm	Energy, µJ	Pulse Spacing, µm	Incision Depth, µm	Numerical Aperture	Flap Detachment	Tissular Bridges
2	1030	2	2	140	0.4	Yes (thanks to the bubble)	Some
		4	2	140		Yes	Some
		4	1	190		Yes	Many
		4	2	190		No	Some
		8	1	190		Yes	None
		8	2	190		Yes (but difficult)	Many
1	1650	2	2	140		Yes	Some
				190		Yes	Some
				140		Yes	None
				140		Yes	None
	1600	1		140		Yes	None

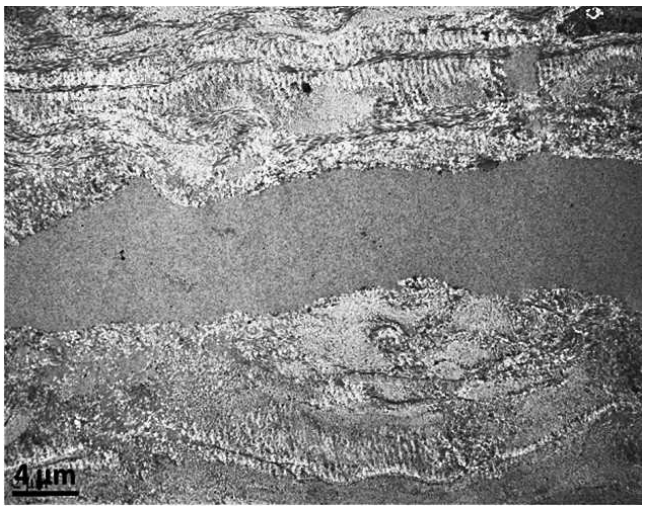

FIGURE 8. Transmission electron micrograph of a lamellar incision performed in the central stroma using a wavelength of 1650 nm and a numerical aperture of 0.57.

Although some variation exists in the data and our observations, the results may be summarized as follows:

- For both wavelength ranges (1030 nm and 1600–1650 nm), pulse energies of 2 µJ and a pulse spacing of 2 µm produced good results for flap thicknesses of 140 µm. Few or no residual tissular bridges remained and the flap detachment was straightforward.
- At 1030 nm, increasing the pulse energy to 4 µJ did not yield significant improvement for 140 µm thick flaps. Higher energies were therefore only tested for 190-µm thick flaps.
- In the longer wavelength range of 1600 nm and 1650 nm, even a lower pulse energy of 1 µJ could be used while still maintaining good incision quality, and easy flap detachment. The slightly shorter wavelength of 1600 nm was chosen in order to reproduce parameters of an alternative compact fiber laser source that has been developed recently by project partners of ours.[26] The difference, if any, between the use of 1650 nm and 1600 nm is that the latter is slightly closer to the water absorption band and would therefore have a slightly smaller penetration depth.

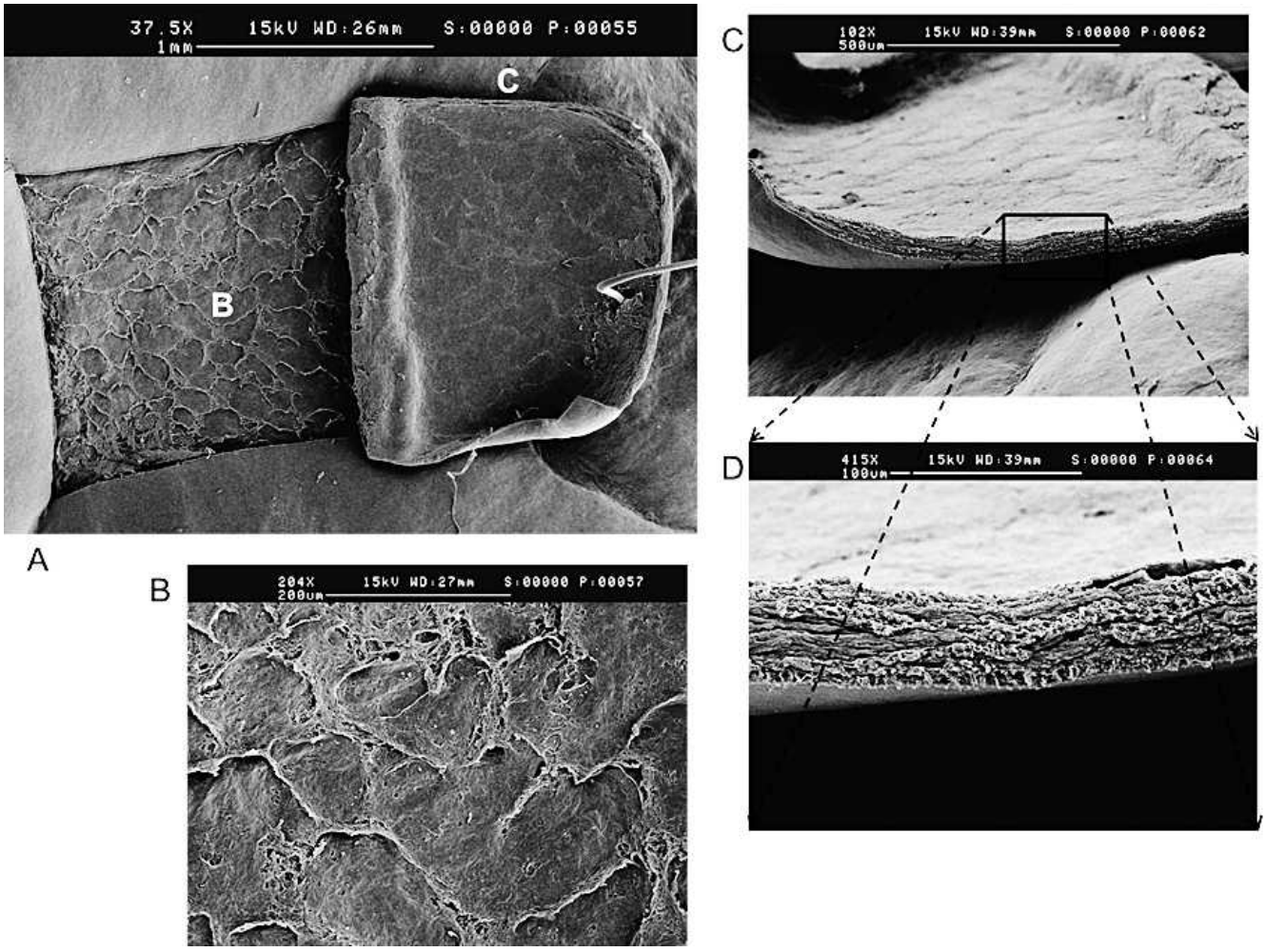

FIGURE 9. Scanning electron micrographs of lamellar cuts performed at 1650 nm using pulse energies of 2 µJ, a numerical aperture of 0.4, and a plot spacing of 2 µm. (**A**) View of the lamellar cut and the flap (×38 magnification). (**B**) Center of the cut surface at higher magnification (×204 magnification). (**C**) Border of the flap (×102 magnification). (**D**) Border of the flap at higher magnification (×415 magnification).

Investigative Ophthalmology & Visual Science

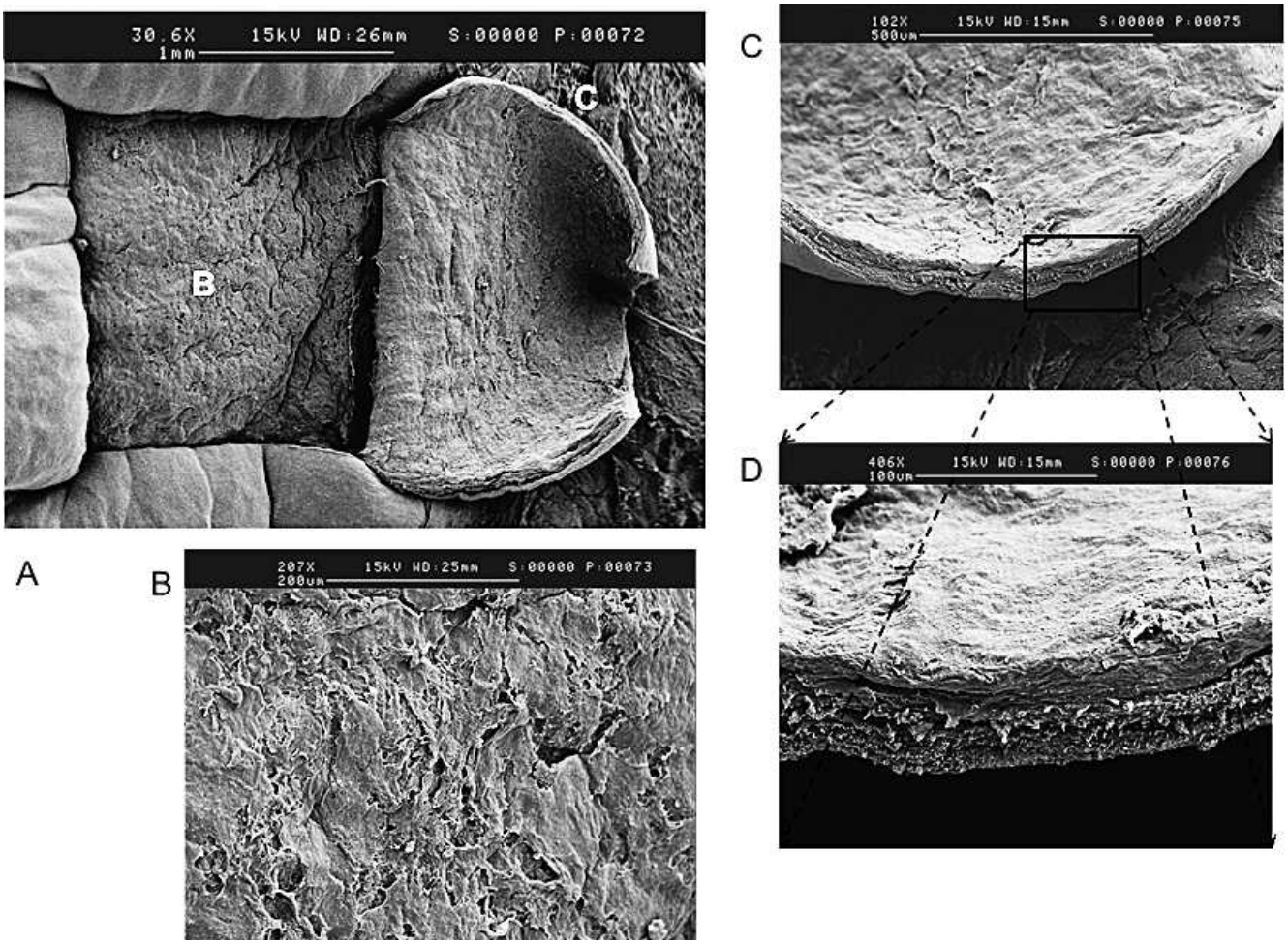

Figure 10. Scanning electron micrographs of lamellar cuts performed at 1030 nm using pulse energies of 4 μJ, a numerical aperture of 0.4, and a plus spacing of 1 μm. (**A**) View of the lamellar cut and the flap (×31 magnification). (**B**) Zoom on the center of the cut surface (×207 magnification). (**C**) Border of the flap (×102 magnification). (**D**) Zoom on the border of the flap (×406 magnification).

- Impeccable flaps were still produced by using the longer wavelength of 1650 nm and 2 μJ pulses spaced at 2 μm at the increased flap depth of 190 μm. No incision could be obtained using 1030 nm with the same pulse parameters.
- Lamellar cut incisions with 1030 nm wavelength pulses required very energetic pulses of 8 μJ and a narrow pulse spacing of 1 μm to obtain easy flap detachment without tissular bridges. Every other possible combination of pulse spacing and lower energy tested resulted in flap detachment difficulties and/or the presence of tissular bridges.

Analysis of the Incision Quality by TEM. As in the optical window centered at 1650 nm, a fraction of the laser energy is transformed into heat by light absorption, the samples were examined in order to verify the possible influence of thermal effects. The analysis of lamellar cuts by transmission electron microscopy confirms the observations made for transfixing cuts. Disrupted tissues and collagen fibers appear structurally unchanged. Figure 8 shows a typical transmission electron micrograph of a lamellar incision, here performed in the anterior stroma using a wavelength of 1650 μm, a numerical aperture of 0.57, and pulse energies of 1.3 μJ, which were just sufficient to create continuous incisions. No thermal side effects are visible around the incision.

Analysis of the Incision Quality by SEM. Parts of the lamellar incisions have been analyzed by SEM. Figures 9 and 10 show scanning electron micrographs of lamellar cuts performed with a numerical aperture of 0.4. We focus here on experimental parameters which are just sufficient to create lamellar incisions of satisfactory quality. Results from the prior section indicate that cuts of similar quality may be obtained with lower required pulse energy (2 μJ instead of 4 μJ) and a wider pulse spacing (2 μm instead of 1 μm) when using a wavelength of 1650 nm versus 1030 nm. While the difference is not striking, the surfaces of the lamellar cut as well as the borders of the transfixing incisions also appear smoother in the case of 1650 nm; the more pronounced roughness observed at 1030 nm may be due to the mechanical rupture of the residual tissular bridges remaining after the laser cut.

Summary and Discussion

Present state-of-the art clinical systems for LASIK and keratoplasty assisted by ultrashort pulse laser use laser sources emitting at wavelengths close to 1000 nm. While these systems have excellent performance in LASIK, their use for keratoplasty is not as straightforward. Performing deep lamellar or penetrating cuts with this type of system can be difficult in typical pathological tissue volumes. These complications may

be attributed to increased light scattering in pathological and particularly edematous corneas.

Our transparency measurements on healthy and edematous corneas reveal a strong light-scattering dependency on the degree of edema and on wavelength. Transparency is optimal for the physiological thickness of the cornea; light scattering considerably increases with increasing thickness and transparency is decreased. However, for any given healthy or edematous cornea, light scattering decreases continually with increased wavelength within the examined visible and SWIR spectral range. When also considering the additional water absorption bands within the SWIR spectral range, a wavelength of optimal transparency centered at 1650 nm may be identified.

Using three laser sources, one of which is simple and compact and may therefore potentially be used in clinical systems, we performed a systematic study of the incision length of penetrating cuts—that is, of the maximum depth in which optical breakdown may be induced for a given pulse energy. By measuring the incision length while varying the energy, the penetration depth of the surgical laser beam may be obtained by fitting the parameters of a Lambert-Beer exponential to the data. The surgical laser beam penetration depth ℓ (the depth at which the radiant exposure has been reduced to $1/e$ of its initial value by light scattering and absorption) is observed to exhibit strong wavelength dependency. While the penetration depth ℓ itself depends strongly on the degree of edema present in the cornea, in all cases a wavelength change from 1030 nm to wavelengths close to 1650 nm typically at least doubles the penetration depth. This is observed despite increased absorption at the longer wavelength.

When changing the wavelength, in theory, the reduction of the spot size by reduced light scattering competes with the broadening of the spot caused by the longer wavelength. If the beams were diffraction limited, the spot surface would be increased by a factor of about 2.6 at the longer wavelength. Were this the case, the correspondingly reduced intensity would be expected to require increasing pulse energy by the same factor to even maintain the threshold radiant exposure at an identical depth, all other parameters unchanged. Instead, the opposite result was observed, indicating that light scattering is in fact the dominant process and that the beam quality was far from diffraction limited even in the case of healthy corneas.

The wavelength change facilitates performing lamellar cuts in the volume of edematous cornea, which is indispensable for femtosecond laser assisted keratoplasty. While the improvement is not significant at depths typical for LASIK, deeper lamellar cuts as necessary for keratoplasty performed at 1600 or 1650 nm require less pulse energy and less narrow spot spacing than those performed at 1030 nm; they considerably facilitate the manual detachment of the flaps or grafts from the rest of the cornea and leave less residual tissular bridges.

Analysis of the incisions by transmission electron microscopy does not reveal any thermal or other side effects induced by the wavelength change. The analysis of lamellar incisions by scanning electron microscopy shows a slight improvement in surface and interface quality when using wavelengths close to 1650 nm. Another welcome benefit of the wavelength change is the fact that wavelengths at and beyond the water absorption peak centered at 1450 nm are inherently "eye-safe" inasmuch as only a negligible amount of the incident light reaches the retina (Table 4).

As a side note, we may remark that the homemade OPG (source 3) requires centering at the optimal transparency of 1650 nm due to its broader emission spectrum to produce the desired effects. Sources with narrower emission spectra may use a wider range of wavelengths of about 1600 to 1700 nm. Experiments in view of controlling the output spectra bandwidth of our sources are currently underway. Our findings did not reveal strong influences of either the numerical aperture (within the range of 0.4–0.57 used here), or the pulse duration on the surgical result.

As far as we know, this is the first study showing that wavelengths in the transparency window centered at 1650 nm are more efficient for obtaining deep cuts on pathological corneas; a significant improvement may even be observed on healthy cornea and may permit use of even lower energies.

Table 4. Quantity of Incident Light on the Cornea Reaching the Crystalline Lens (4 mm of Water Separating Those Two Tissues) and the Quantity Reaching the Retina Considering 22 mm of Water Separating Those Two Tissues at Different Wavelengths

Wavelength, nm	Incident Light on Cornea Reaching the Anterior Surface of the Crystalline Lens, %	Incident Light on Cornea Reaching the Retina, %
830	99	93
1030	93	67
1300	65	9.4
1650	13	0.01

Acknowledgments

The authors thank the French Eye Bank for the supply of human corneas. Doctoral scholarships were obtained from the *Direction Générale de l'Armement* (FD) and the Centre National de la Recherche Scientifique (CC). We thank Virginie Garnier-Thibaud, Service de Microscopie Électronique, Institut de Biologie Intégrative IFR 83, Université Pierre et Marie Curie – Paris VI, for providing the SEM data on incised corneas. We thank Bob L. Zimering for help with the manuscript.

Supported by the Agence Nationale de la Recherche (GRECO project, ANR-06-TecSan-025, NOUGAT project, ANR-08-TecSan-012).

Disclosure: **C. Crotti**, None; **F. Deloison**, None; **F. Alahyane**, None; **F. Aptel**, None; **L. Kowalczuk**, None; **J.-M. Legeais**, None; **D.A. Peyrot**, None; **M. Savoldelli**, None; **K. Plamann**, None

References

1. Vogel A, Noack J, Hüttman G, Paltauf G. Mechanisms of femtosecond laser nanosurgery of cells and tissues. *Appl Phys B*. 2005;81:1015–1047.
2. Stern D, Schoenlein RW, Puliafito CA, Dobi ET, Birngruber R, Fujimoto JG. Corneal ablation by nanosecond, picosecond, and femtosecond lasers at 532 and 625 nm. *Arch Ophthalmol*. 1989;107:587–592.
3. Sletten KR, Yen KG, Sayegh S, et al. An in vivo model of femtosecond laser intrastromal refractive surgery. *Ophthalmic Surg Las*. 1999;30:742–749.
4. Juhasz T, Kastis GA, Suárez C, Bor Z, Bron WE. Time-resolved observations of shock waves and cavitation bubbles generated by femtosecond laser pulses in corneal tissue and water. *Lasers Surg Med*. 1996;19:23–31.
5. Juhasz T, Loesel FH, Horvath C, Bille JF, Mourou G. Corneal refractive surgery with femtosecond lasers. *IEEE J Sel Top Quantum Electron*. 1999;5:902–910.
6. Kurtz RM, Horvath C, Liu HH, Krueger RR, Juhasz T. Lamellar refractive surgery with scanned intrastromal picosecond and femtosecond laser pulses in animal eyes. *J Refract Surg*. 1998; 14:541–548.

7. Loesel FH, Niemz MH, Bille JF, Juhasz T. Laser-induced optical breakdown on hard and soft tissues and its dependence on the pulse duration: experiment and model. *IEEE J Quantum Electron*. 1996;32:1717–1722.
8. Horvath C, Braun A, Liu H, Juhasz T, Mourou G. Compact directly diode-pumped femtosecond Nd: glass chirped-pulse-amplification laser system. *Opt Lett*. 1997;22:1790–1792.
9. Binder P. Femtosecond applications for anterior segment surgery. *Eye Contact Lens*. 2010;36:282–285.
10. Juhasz T, Loesel FH, Kurtz RM, Horvath C, Billy JF, Mourou G. Corneal refractive surgery with femtosecond lasers. *IEEE J Sel Top Quantum Electron*. 1999;5:902–910.
11. Salomão MQ, Wilson SE. Femtosecond laser in laser in situ keratomileusis. *J Cataract Refr Surg*. 2010;36:1024–1032.
12. Soong HK, Malta JB. Femtosecond lasers in ophthalmology. *Am J Ophthalmol*. 2008;147:189–197.
13. Plamann K, Aptel F, Arnold C, et al. Ultrashort pulse laser surgery of the cornea and the sclera. *J Opt*. 2010;12:084002.
14. Buratto L, Böhm E. The use of the femtosecond laser in penetrating keratoplasty. *Am J Ophthalmol*. 2007;144:975–976.
15. Sikder S, Snyder RW. Femtosecond laser preparation of donor tissue from the endothelial side. *Cornea*. 2006;25:416–422.
16. Binder PS, Sarayba M, Ignacio T, Juhasz T, Kurtz R. Characterization of submicrojoule femtosecond laser corneal tissue dissection. *J Cataract Refract Surg*. 2008;34:146–152.
17. Olivié G, Diguère D, Vidal F, et al. Wavelength dependence of femtosecond laser ablation threshold of corneal stroma. *Opt Express*. 2008;16:4121–4129.
18. Farrell RA, McCally RL, Tatham PE. Wave-length dependencies of light scattering in normal and cold swollen rabbit corneas and their structural implications. *Physiol*. 1973;233:589–612.
19. Farrell RA, McCally RL. On corneal transparency and its loss with swelling. *J Opt Soc Am*. 1976;66:342–345.
20. Sacks ZS, Kurtz RM, Juhasz T, Spooner G, Mourou GA. Subsurface photodisruption in human sclera: wavelength dependence. *Ophthalmic Surg Lasers Imaging*. 2003;34:104–113.
21. Sacks ZS, Kurtz R, Juhasz T, Mourou GA. Femtosecond subsurface photodisruption in scattering human tissues using long infrared wavelengths. *Proc SPIE*. 2001;4241:98–111.
22. Peyrot DA, Aptel F, Crotti C, et al. Effect of incident light wavelength and corneal edema on light scattering and penetration: laboratory study of human corneas. *J Refr Surg*. 2010;26:786–795.
23. van den Berg T, Spekreijse H. Near infrared light absorption in the human eye media. *Vis Res*. 1997;37:249.
24. Nuzzo V, Plamann K, Savoldelli M, et al. In situ monitoring of second harmonic generation in human corneas to compensate for femtosecond laser pulse attenuation applied to keratoplasty. *J Biomed Opt*. 2007;12:064032.
25. Nuzzo V, Aptel F, Savoldelli M, et al. Histologic and ultrastructural characterization of corneal femtosecond laser trephination. *Cornea*. 2009;28:908–913.
26. Morin F, Druon F, Hanna M, Georges P. Microjoule femtosecond fiber laser at 1.6 μm for corneal surgery applications. *Opt Lett*. 2009;34:1991–1993.

Investigative Ophthalmology & Visual Science